



## A procedure for extracting primary and secondary creep parameters from nanoindentation data



J. Dean<sup>a</sup>, A. Bradbury<sup>a</sup>, G. Aldrich-Smith<sup>b</sup>, T.W. Clyne<sup>a,\*</sup>

<sup>a</sup> Department of Materials Science & Metallurgy, Cambridge University, Pembroke Street, Cambridge CB2 3QZ, UK

<sup>b</sup> AWE, Aldermaston, Reading, Berkshire RG7 4PR, UK

### ARTICLE INFO

#### Article history:

Received 14 October 2012

Received in revised form 28 January 2013

Available online 21 June 2013

#### Keywords:

Nanoindentation

Finite element analysis

Creep

Non-destructive testing

### ABSTRACT

A methodology is presented for the extraction of creep parameters from nanoindentation data – i.e. data obtained from an indentation system with a high resolution displacement measuring capability. The procedure involves consideration of both primary and secondary creep regimes. The sensitivities inherent in the methodology are explored and it is concluded that, provided certain conditions are satisfied, it should be reasonably robust and reliable. In contrast to this, it is also shown that the methodology commonly used at present to obtain (steady state) creep parameters is in general highly unreliable; the effects responsible for this are identified.

© 2013 Elsevier Ltd. All rights reserved.

### 1. Introduction

The stress and strain fields within a specimen during indentation are complex, for all indenter shapes, even if it's assumed that the material (and also the scale of the indenter tip, the nature of any oxide film at the surface etc.) are such that it can be treated as an isotropic continuum. While the measured outputs (load–displacement–time relationships) are dependent on the constitutive relations characterising the material behaviour, inferring these relations from such output data presents major challenges. In fact, provided the testing can be done under conditions such that creep has a negligible influence on the characteristics being measured, it is possible to extract both the yield stress and the (initial) work-hardening rate from experimental indentation data, using FEM modelling, in a fairly tractable and straightforward way. Dean et al. (2010a) recently presented recommendations about how to optimise these procedures, concluding that the yield stress can typically be estimated with an accuracy of around  $\pm 10\%$  and the work hardening rate to about  $\pm 25\%$ . This is clearly a very useful capability, which is likely to

be exploited increasingly in the future. A subsequent paper (Dean et al., 2010b) explored the scope for deducing residual stress levels in surface layers from indentation data, concluding that, while this can also be done (provided the yield stress is known to a high precision), the accuracy is unlikely to be better than about  $\pm 50\%$ .

In practice, creep effects often exert a strong influence on the indentation response, even when testing is carried out at ambient temperature. As an example of this influence, it is common to impose a 'dwell period' at constant (peak) applied load, during which progressive penetration occurs. If this is not done, then the initial unloading gradient is often found to be non-linear, and Young's modulus values derived from this gradient then tend to be inaccurate. The dwell period is regarded as allowing creep effects (under the load concerned) to diminish until they become acceptably small. Some attempts have been made to quantify this. For example, Chudoba and Richter (2001) suggested that the period should be long enough for the depth increase occurring in one minute to be less than one percent of the current depth.

In fact, there has been extensive recognition of the potential significance of creep during indentation, both as a factor that might complicate the extraction of plastic or elastic characteristics (Chudoba and Richter, 2001; Seltzer

\* Corresponding author.

E-mail address: [twc10@cam.ac.uk](mailto:twc10@cam.ac.uk) (T.W. Clyne).

and Mai, 2008) and also in terms of the scope for obtaining creep parameters from indentation data (Stone et al., 2010; Galli and Oyen, 2009; Cao, 2007). Various procedures have been proposed for evaluation of creep parameters. However, it is fairly clear that none of them represent universally robust or reliable methodologies, and several papers have highlighted this point (Goodall and Clyne, 2006; Chen et al., 2010).

A prime cause for this lack of reliability is that most proposed methodologies tend to focus on steady state (stage II) creep, with the assumption being (explicitly or implicitly) made that the influence of primary creep can somehow be eliminated from the measurements. Unfortunately, while this is easily done during conventional (uniform stress field) testing, it is virtually impossible during indentation testing, since regions of the specimen undergoing primary creep are continually entering the creep strain field (and influencing the indenter displacement response). This difficulty has been recognised in a general sense by some workers (Takagi et al., 2008; Stone and Elmustafa, 2008), and extensive FEM studies have been carried out to study stress and strain fields, but the emphasis has always tended to be on the idea that some sort of “quasi-steady state” does become established (fairly quickly), and that measurements yielding (stage II) creep parameters can be made in this regime.

One of the difficulties here is that a “creep indentation curve” (displacement history during a constant load “dwell”) often exhibits a (short) initial transient followed by a regime of approximately constant penetration rate, which is very reminiscent of “stage II” in a creep strain history obtained during conventional (uniform stress field) testing. However, in reality the system is not in any sense conforming to a steady state in this regime. The stress and strain field under the indenter are continually changing and local regions are constantly moving along their own creep strain history curves (with many regions inevitably being in the early – i.e. primary – part of the curve, even after an extended period of indentation). There is no requirement that the resultant indenter displacement history should be linear at any stage, although it’s certainly possible that it could be at least approximately linear.

If attempts are made to treat an indenter displacement history as if it were a creep strain history, problems immediately arise with identifying a (unique) strain, and hence strain rate, after any specified time, and also a representative stress. The effective strain rate is often taken to be the penetration rate divided by the current depth, while an “equivalent” stress was defined by Mulhearn and Tabor (1960) as the applied load divided by the projected contact area. However, there is really no justification whatsoever for representing the actual situation as if it corresponded to a uniformly loaded sample experiencing these stresses and strains, particularly since primary creep typically generates much higher (and more variable) strain rates than secondary creep (under the same applied stress) – i.e. the sensitivities governing creep behaviour are such that making such an assumption is likely to cause massive errors. Indeed, while there have not been many publications specifically highlighting the unreliability of such procedures for extracting creep parameters from indentation data, most researchers in the field are well aware of the difficulties.

Of course, there have been reports of successful measurement of creep parameters via indentation. Fujiwara and Otsuka (2001) focussed on the “steady state” part of the creep dwell curve and hence derived  $n$  (stress exponent) and  $Q$  (activation energy) for a eutectic Sn–Pb alloy, reporting good agreement with values obtained by conventional creep testing. Liu et al. (2007a) used a similar approach to obtain  $n$  for Mg–Sn alloys. Liu et al. (2007) also reported good agreement between values of  $n$  for an Al alloy obtained via uniaxial creep tests (between 212 MPa and 246 MPa, at 200 °C), which gave  $n = 5.3$ , and via indentation (at fixed loads corresponding to ‘representative’ stresses between 905 MPa and 1415 MPa, also at 200 °C), which gave  $n = 4.9$ . Such agreement is surprising in view of the large difference in stress levels between the two types of test, and also since a stress of 1.4 GPa would be expected to induce high levels of damage in Al. Changes in creep mechanism would certainly be likely if the stress were to change over such a large range.

It’s also worth noting that, as pointed out by Goodall and Clyne (2006), most studies in which good correlation has been reported between creep parameters obtained by indentation and by uniaxial testing were carried out on materials that creep rapidly at room temperature – notably Pb, Sn and In. In such materials, which exhibit very high stage II creep rates, the effects of primary creep, and the sensitivity to changes in creep mechanism, may be less pronounced than with more creep-resistant materials.

In the present paper, a procedure is described in which full account is taken of the nature of the stress and strain histories experienced by local regions under the indenter, and the consequences for its displacement characteristics. A methodology is presented for extracting creep parameters defining the complete (primary plus secondary) creep curve, dependent only on a suitable functional form being established for it.

## 2. Experimental procedures

### 2.1. Material

The experimental work has been conducted on OFHC extruded copper rod, in as-received form. The material is the same as that employed in a previous study (Dean et al., 2010a), which was focussed on obtaining the yield stress and work hardening rate from indentation data. Information is provided there about the preparation procedures, microstructure etc. In the previous study, it was shown that more consistent data are obtained when the indent straddles several grains, rather than being located within a single grain, and it was therefore ensured that such “multi-grain” interrogation was being carried out in all of the tests described here. All tests involved compressive loading in the axial (extrusion) direction of the copper rod.

### 2.2. Uniaxial compression testing to obtain stress–strain data

The macroscopic stress–strain behaviour of the copper was characterised using conventional mechanical testing procedures. Cylinders (8 mm height, 6 mm diameter) were

compressed in the axial direction between flat platens of silicon carbide, under displacement control ( $0.1 \text{ mm s}^{-1}$ ), using a 10 kN ESH servo-hydraulic mechanical test machine. The ends were lubricated with molybdenum disulphide, to minimise barreling. Displacements were measured using a Linear Variable Displacement Transducer (LVDT). For testing at elevated temperatures, specimens were enclosed within a furnace. Yield stresses and (initial) work-hardening rates were obtained at 25 °C, 50 °C, 100 °C and 150 °C. As can be seen in Table I, the yield stress ranged from 286 MPa at 298 K to 265 MPa at 423 K.

### 2.3. Uniaxial compression testing to obtain creep data

Macroscopic creep tests (over a range of temperature and stress) were conducted in compression, using a customised loading arrangement. Cylinders (4 mm diameter, 5 mm height), with lubricated ends, were compressed between (heated) flat platens of hardened steel, using static weights to generate the load. Displacements were measured using a scanning laser extensometer, with an accuracy of  $\pm 1 \mu\text{m}$ . These tests were carried out at 4 temperatures, with stress levels ranging from 82 MPa up to 182 MPa, the latter representing a substantial proportion of the yield stress.

### 2.4. Indentation procedure

Indentation testing was carried out using a pendulum-based nanoindenter (MicroMaterials Ltd) housed in a vacuum chamber. Tests were carried out under vacuum, using a spherical diamond indenter (nominally  $10 \mu\text{m}$  radius), with the indentation direction parallel to the extrusion axis of the copper bar, at temperatures of 25 °C, 50 °C, 100 °C and 150 °C. Both specimen and tip were heated, in order to minimise thermal drift – see below.

Tests were carried out with loading rates of 0.1, 0.5, 3.0, 10.0, and  $20.0 \text{ mN s}^{-1}$  (with 3 indents made at each loading rate), until a prescribed depth of  $2 \mu\text{m}$  had been attained. The maximum load required to reach this depth is dependent on the material response (including its creep response). Once this depth had been reached, the load at that point was held constant for a specified period (3600 s) – the creep dwell period – before the indenter was retracted at an unloading rate of  $20 \text{ mN s}^{-1}$ .

Considerable attention was paid to thermal drift, which is potentially of some significance in creep studies, particularly during extended loading (such as the 1 h dwells used in the current work). It is, of course, important to separate thermal drift effects from displacements due to specimen deformation (creep). On the other hand, thermal drift

**Table I**

Measured values of the yield stress and (initial) work-hardening rate of copper samples, for the four temperatures employed.

Temperature (K)	Yield stress (MPa)	Work hardening rate (MPa)
298	286	312
323	280	235
373	275	211
423	265	128

measurements made using a set-up from which the specimen had been removed could be misleading as a consequence of the altered thermal environment. This issue was addressed by measuring the thermal drift rate with a tungsten specimen in place, having the same dimensions as the copper samples. The thermal conductivity of tungsten is relatively high (about half that of Cu), so that the thermal environment would be similar in the two cases, while the tungsten is expected to be effectively immune from creep over the range of temperature concerned. The thermal drift rate was measured at the highest temperature (150 °C), with the applied force having been reduced to 10% of the maximum, during the unloading phase. The drift rate was found to be constant at  $\sim 0.02 \text{ nm s}^{-1}$  over a period of an hour, and this rate appeared to be characteristic of the physical set-up over the range of temperatures employed in the present work. All displacement data were therefore corrected for this thermal drift, the correction being relatively small, but not insignificant – particularly for the dwell at constant load.

The system compliance was established using high load indentations on three reference materials, namely single crystal tungsten, a tool steel and fused silica. Data are presented after correction for this compliance.

## 3. FEM modelling

### 3.1. Mesh formulation and boundary condition specification

An axisymmetric finite element model was built using ABAQUS commercial software. The specimen was modelled as a deformable body and meshed with 5625 linear

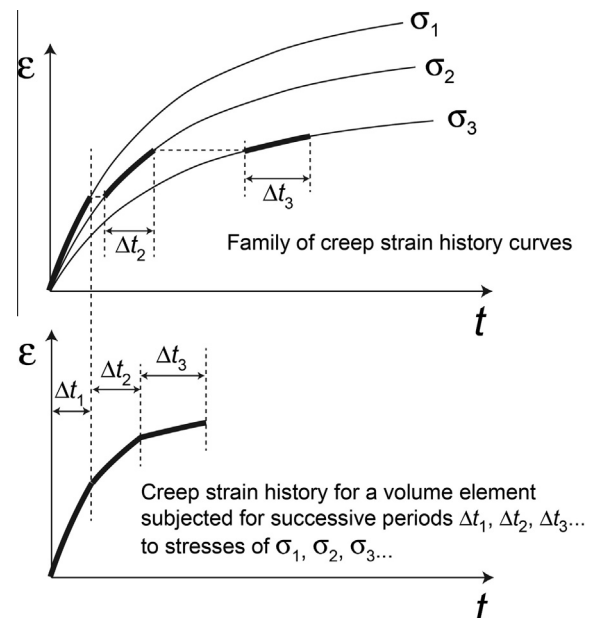


**Fig. 1.** Schematic illustration of how the creep strain history of a volume element is assumed to be composed of a series of incremental strains, each dependent on the creep curve for the stress level concerned and the prior cumulative creep strain experienced by the element.

quadrilateral (hybrid) elements (type CAX4H). The indenter was modelled as an analytical rigid body. The mesh was refined directly beneath the indenter, in order to improve the resolution in this region. A sensitivity analysis confirmed that this mesh was sufficiently fine to achieve convergence, numerical stability and mesh-independent results. (The same mesh was used in an earlier paper (Dean et al., 2010a), where is it described more fully.)

Experimental displacement histories, for each of the loading rates, were specified as a boundary condition. The load at the point when the indenter depth reached 2  $\mu\text{m}$  was an output of the modelling, dependent on the material response (i.e. its yielding and creep characteristics). In a sec-

ond set of simulations, experimental load histories, for each of the loading rates, were specified as a boundary condition. The indenter displacement at the end of the dwell period was an output of the modelling, dependent on the material response. The predicted displacement of the indenter during the creep dwell period was continuously output, for comparison with experimental data.

If the procedure were being applied to a material with unknown creep characteristics, then the algorithm for obtaining them would consist of iterative refinement to the creep parameters, such that optimum agreement was reached between predicted and measured load–displacement–time relationships. In the present work, some

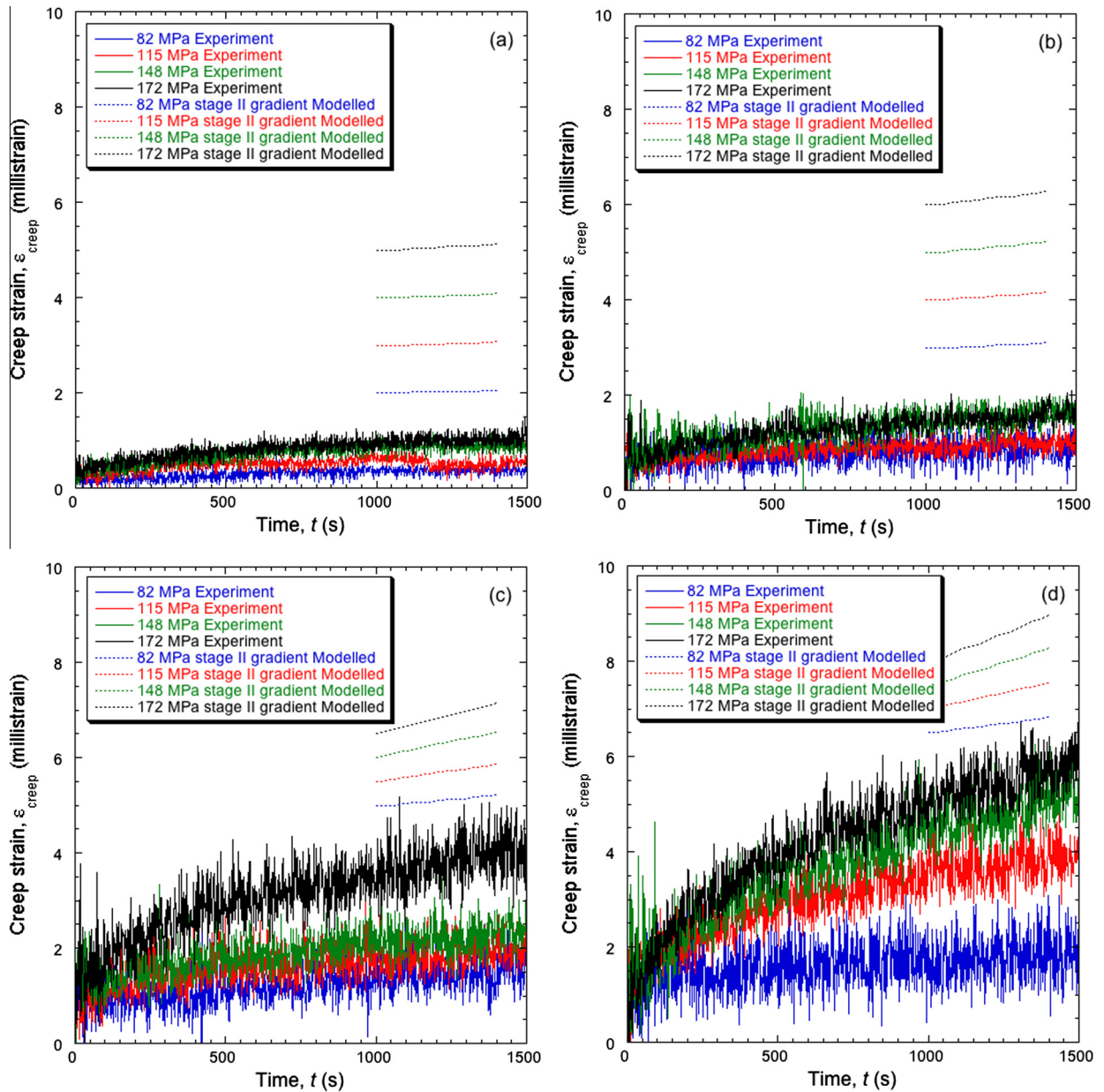


Fig. 2. Experimental creep strain data from conventional compression testing, at temperatures of (a) 298 K, (b) 348 K, (c) 423 K and (d) 473 K. Also shown are corresponding modelled stage II strain rates, obtained using Eq. (2) with parameter values of  $A = 3.79 \cdot 10^{-8} \text{ MPa}^{-n} \text{ s}^{-1}$ ,  $n = 1.47$  and  $Q = 13.4 \text{ kJ mol}^{-1}$ .

iteration was employed, but this was fairly limited, and data obtained during the conventional creep testing were used to identify the regime of parameter values in which this was carried out.

### 3.2. Constitutive relations

#### 3.2.1. Plasticity

Measured values of the yield stress (0.2% proof stress) and (initial) work-hardening rate, as a function of temperature, are presented in Table I. Both were found to decrease with increasing temperature in an approximately linear fashion. The constitutive plasticity relation was assumed to take the following form:

$$\sigma(T) = \sigma_V(T) + k(T)\varepsilon_{pl} \quad (1)$$

where  $\varepsilon_{pl}$  is the equivalent plastic strain and  $k$  is the work-hardening rate.

#### 3.2.2. Creep

Two constitutive creep laws were employed. The first was the conventional steady-state creep law, expressed as a strain rate

$$\frac{d\varepsilon_{creep}}{dt} = A\sigma^n \exp\left(\frac{-Q}{RT}\right) \quad (2)$$

in which  $A$  is a constant (units of  $s^{-1} MPa^{-n}$ ),  $n$  is the stress exponent,  $Q$  is the activation energy ( $J mole^{-1}$ ),  $R$  is the universal gas constant and  $T$  is the absolute temperature. This was implemented in ABAQUS using the user subroutine \*CREEP. Values for  $A$ ,  $n$  and  $Q$  were obtained from the macroscopic creep tests (§2.3). It was assumed that, in any volume element, the creep rate given by Eq. (2), for the local (deviatoric) stress (and temperature) concerned, is instantaneously adopted at any point during the test. (Of course, the local stress in a volume element changes continuously, in a way that is dictated by the applied load, loading geometry and constraint imposed by the presence of all the other volume elements.)

The second creep relationship employed was one representing the complete creep strain history (primary + secondary regimes), sometimes termed the Miller–Norton law,

$$\varepsilon_{creep} = \frac{C\sigma^n t^{m+1}}{m+1} \exp\left(\frac{-Q}{RT}\right) \quad (3)$$

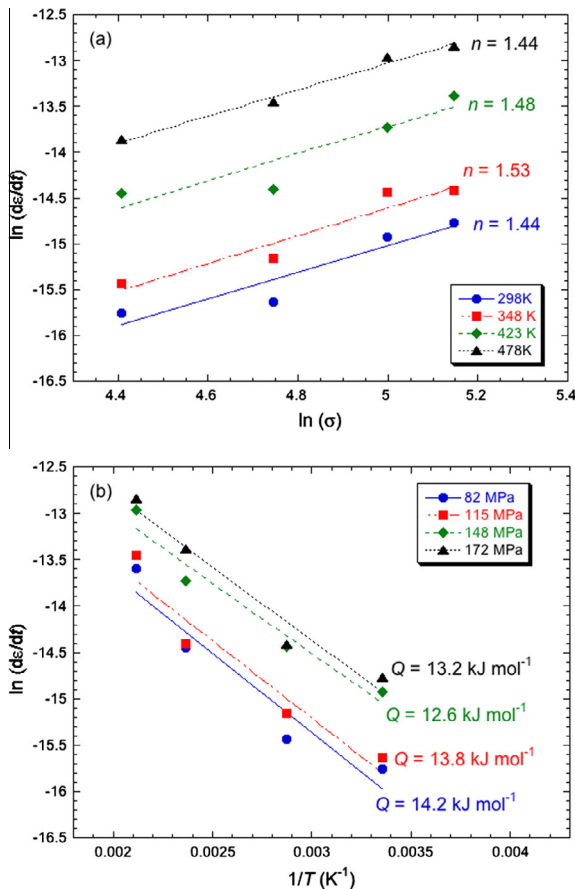


**Fig. 3.** Plots of the natural logarithm of the strain rate in stage II, as measured in conventional creep tests, against (a) the log of the applied stress (in MPa) and (b) the reciprocal of the absolute temperature, showing how estimates of the stress exponent and the activation energy were obtained.

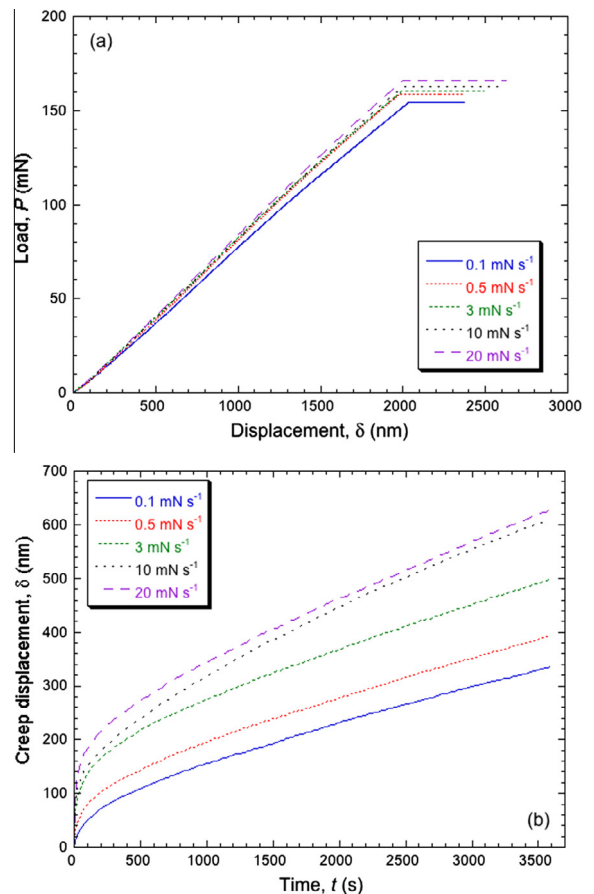


**Fig. 4.** Experimental indentation data obtained at ambient temperature ( $T = 298 K$ ), showing (a) load–displacement plots during both the build-up of the load and the dwell, and (b) displacement histories during the dwell, for five different loading rates during the build-up.

in which  $C$  is a constant (units of  $\text{MPa}^{-n} \text{s}^{-(m+1)}$ ),  $t$  is the time (s) and  $m$  is a dimensionless constant. The values of the parameters in this expression were obtained by iterative fitting to the measured uniaxial creep strain histories. The same thing was also done for the indentation test data, with the fitting being carried out in terms of the load required to penetrate  $2 \mu\text{m}$ , and the displacement during the dwell, both as a function of loading rate.

It's important to note how Eq. (3) was applied in order to obtain the increments of strain generated in a given volume element as it experienced a changing (deviatoric) stress throughout the test. The equation can be differentiated with respect to time, to give

$$\frac{d\epsilon_{\text{creep}}}{dt} = C\sigma^n t^m \exp\left(\frac{-Q}{RT}\right)$$

The time can thus be expressed in terms of both strain rate and strain.

$$t = \left[ \frac{\frac{d\epsilon_{\text{creep}}}{dt}}{C\sigma^n \exp\left(\frac{-Q}{RT}\right)} \right]^{1/m} = \left[ \frac{(1+m)\epsilon_{\text{creep}}}{C\sigma^n \exp\left(\frac{-Q}{RT}\right)} \right]^{1/(1+m)}$$

Eliminating  $t$  and rearranging allows the strain rate to be expressed as a function of the strain

$$\frac{d\epsilon_{\text{creep}}}{dt} = \left[ C\sigma^n \exp\left(\frac{-Q}{RT}\right) \{ (1+m)\epsilon_{\text{creep}} \}^m \right]^{1/(1+m)} \quad (4)$$

The manner in which successive increments of strain were established, as indentation continued (and the stress within the volume element changed) is illustrated in Fig. 1. As can be seen, it was assumed that the cumulative creep strain defines the ‘state’ of (a volume element of) the material. The instantaneous creep strain rate was then defined by the current stress (in the volume element concerned) and the prior strain: the creep strain rate thus has no explicit dependence on time.

#### 4. Steady state creep parameters from uniform stress field testing

Experimental creep strain histories, for the temperatures and stress levels employed, are shown in Fig. 2. Also shown on these plots are the corresponding (steady state) creep strain history gradients, obtained using Eq. (2) with best fit values of  $A$  ( $3.79 \cdot 10^{-8} \text{MPa}^{-n} \text{s}^{-1}$ ),  $n$  (1.47) and  $Q$  ( $13.4 \text{kJ mol}^{-1}$ ). These values of  $n$  and  $Q$  were obtained as average gradients of the plots shown in Fig. 3, where it can be seen that there is a reasonable degree of internal consistency – i.e. the data do lie on approximately straight lines, as expected. It's a little difficult to say whether these values of  $Q$  and  $n$  are of the magnitude expected. They are both relatively low. However, it's worth noting that these tests were carried out at relatively low homologous temperatures ( $\sim 0.3$ ), where diffusion through low resistance pathways (dislocations and grain boundaries) might be expected to dominate over lattice diffusion: this is certainly expected to give rise to a relatively low value for  $Q$ , and possibly for  $n$  as well.

### 5. Creep parameters from indentation using a “steady state” assumption

#### 5.1. Indentation data

Indentation data obtained at 298 K are presented in Fig. 4. Fig. 4(a) shows load–displacement curves, for several different loading rates. These curves include the dwell period. (The unloading portions have been removed, for clarity.) There are two noteworthy points. The first concerns the load required to reach the specified indentation depth of  $2 \mu\text{m}$ . This decreases with decreasing loading rate. This can be attributed to creep deformation occurring during loading (with simultaneous plasticity). The effect is more pronounced with a low loading rate, since the time to reach the specified depth is then longer. For instance, at 298 K, the time to reach  $2 \mu\text{m}$  at  $0.1 \text{mN s}^{-1}$  is  $\sim 1500 \text{s}$ , whereas at  $20 \text{mN s}^{-1}$  it only takes  $\sim 8 \text{s}$ .

The second point to note concerns the continued penetration of the indenter into the specimen at constant load during the dwell period, shown in Fig. 4(b). This regime corresponds to the horizontal portions in Fig. 4(a). When

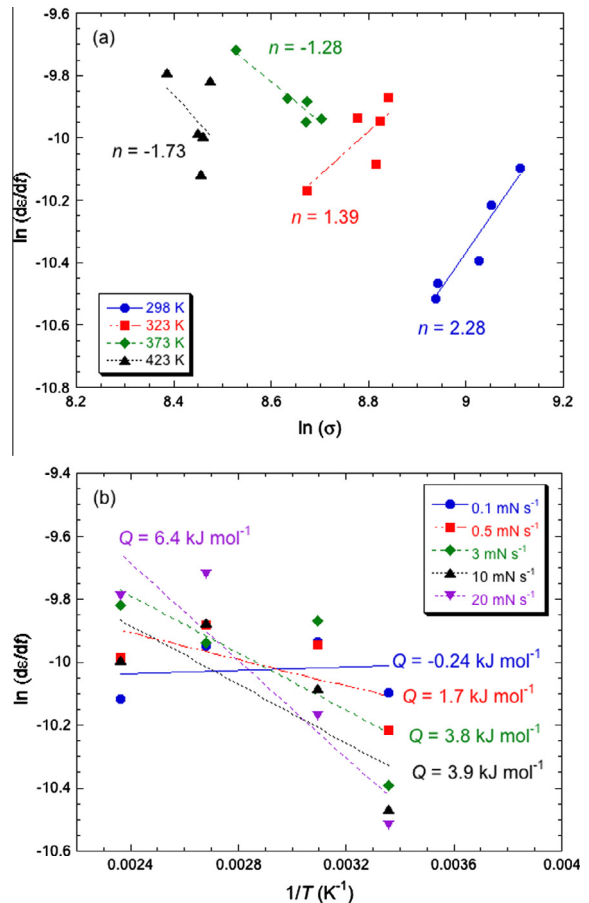


Fig. 5. Plots of the natural logarithm of the apparent strain rate in stage II, as obtained in indentation tests, against (a) the log of the “equivalent” stress (in MPa) and (b) the reciprocal of the absolute temperature, showing how attempts were made to estimate the stress exponent and the activation energy.

the loading rate to 2  $\mu\text{m}$  depth is low, the displacement of the indenter (during the dwell period of 1 h) is less than that for higher initial loading rates. This is consistent with there being a greater creep contribution during the loading phase at low loading rates, leading to greater relaxation of the stresses. The driving force for continued creep during the dwell period is thus reduced. When the 2  $\mu\text{m}$  depth was reached at low loading rates, the indenter thus continued to penetrate to a lesser degree than when the 2  $\mu\text{m}$  depth was reached at a higher loading rate.

## 5.2. Steady-state creep analysis

There is a commonly-employed methodology for obtaining steady-state creep parameters from indentation

data of the type shown in Fig. 4(b). It is based on assuming a uniform stress, strain and strain rate beneath the indenter, with the strain rate being taken as equal to  $(1/h)(dh/dt)$ , where  $h$  is the depth and  $dh/dt$  is the velocity of indenter displacement in the linear region of the displacement–time curve – it can be seen in Fig. 4(b) that the plots do exhibit approximately linear regions. As outlined earlier, these assumptions are likely to be highly unreliable. In fact, it's unclear whether much, or indeed any, of the deforming volume will have entered the secondary (steady state) creep regime during the test. It's worth noting that most such measurements have hitherto been carried out over relatively short timescales.

Notwithstanding these causes for concern, this “standard” procedure was carried out, with the indenter velocity

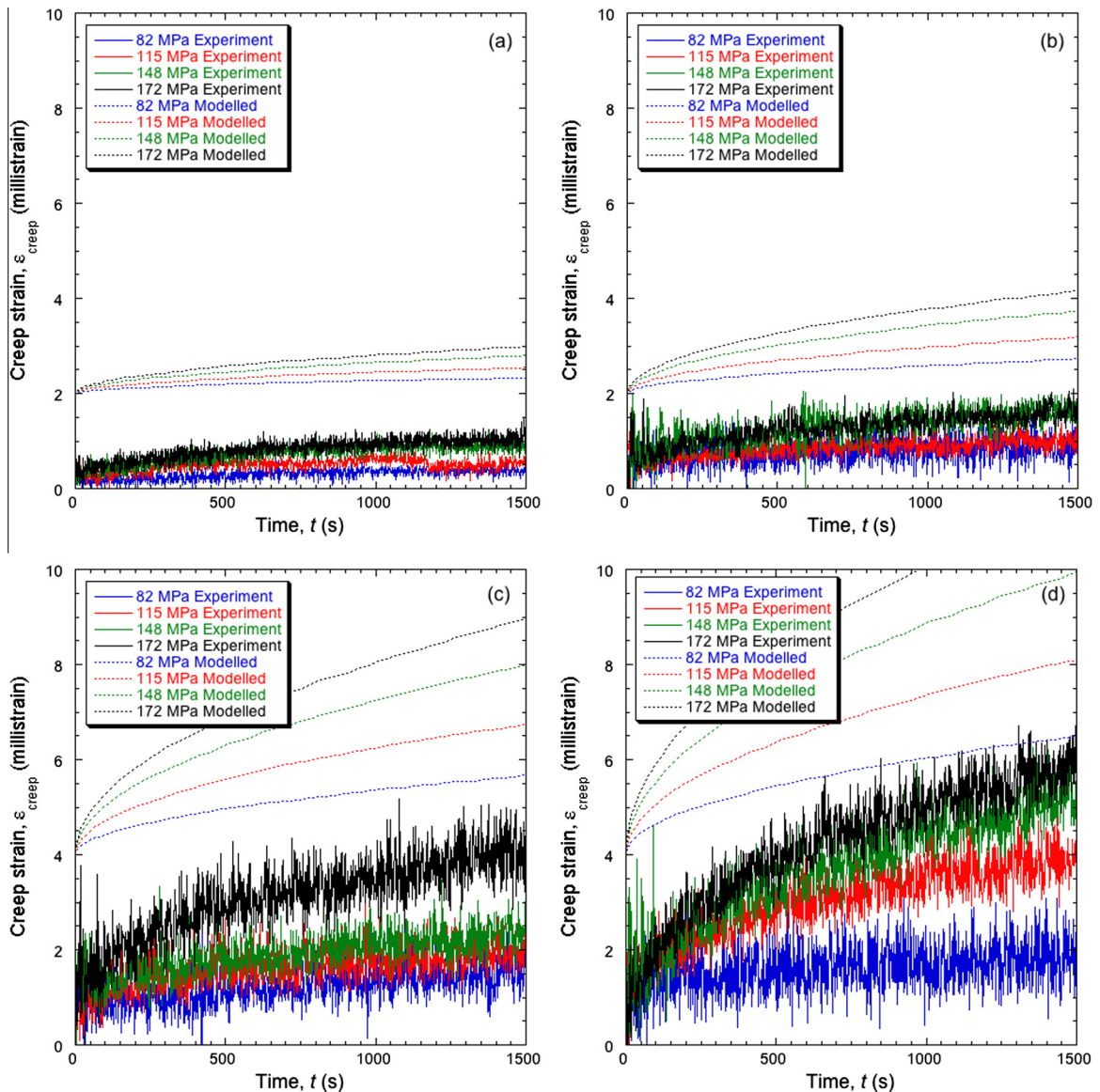


**Fig. 6.** Experimental creep strain data from conventional compression testing, at temperatures of (a) 298 K, (b) 348 K, (c) 423 K and (d) 473 K. Also shown are corresponding modelled creep histories, obtained using Eqn.(3) with parameter values of  $C = 1.5 \cdot 10^{-6} \text{ MPa}^{-n} \text{ s}^{-(m+1)}$ ,  $m = -0.5$ ,  $n = 1.47$  and  $Q = 13.4 \text{ kJ mol}^{-1}$ . (The modelled curves are offset along the creep strain axis, for clarity.).

being evaluated from the approximately linear parts of the curves in Fig. 4(b), and applied for all loading rates, temperatures and “equivalent stresses”. These data are presented in Fig. 5. It’s clear from these plots that any attempt to determine the steady-state creep parameters in this way will be highly unreliable. The values obtained for  $n$  range from about  $-2$  to  $+2$ , while  $Q$  values vary between  $\sim 0$  and  $6 \text{ kJ mole}^{-1}$ . Moreover, these values have been obtained by plotting linear fits through data that exhibit little or no correlation, and it’s clear that there can be no confidence at all in the procedure.

**6. Creep parameters from indentation under unsteady conditions**

*6.1. Functional representation of the complete creep strain curve*

The main source of error in the procedure of §5.2 is fairly clear. Primary creep is evidently having a strong influence on the observed behaviour, even after extended periods of indentation, and any analysis that takes no account of this is likely to be highly unreliable. This is unsurprising, since creep rates at the start of the primary regime are typically greater than those in the steady state regime by something like 1–2 orders of magnitude. This is illustrated by the data in Fig. 6. For example, from the modelled plots (extrapolating beyond the times shown in Fig. 6), the creep rate after one minute is about 25 times greater than that after 10 h, for  $m = -0.5$ .

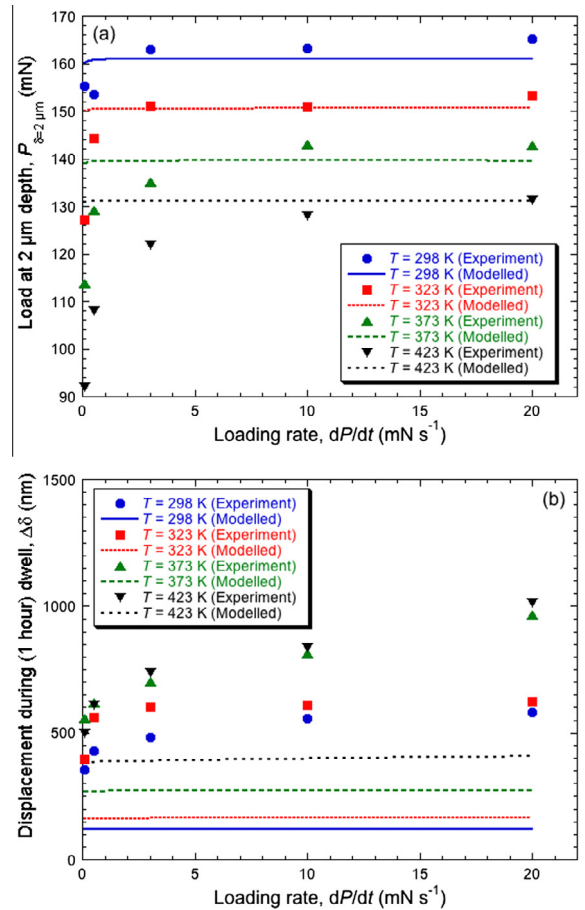
In order to incorporate the effect of primary creep in a comprehensive model algorithm, a functional representation is required for the complete creep strain history – or at least for the portion of interest, which would commonly include the whole of the primary part of the curve and extend into stage II. In the present work, this has been done using Eq. (3). Of course, other functional forms could be used, but all of them are likely to be more or less empirical and the only issue of significance here is whether the actual (macroscopic) behaviour of the material can be well-captured by the expression concerned, using best fit values of the parameters.

Fig. 6 shows the creep curves obtained by conventional compression testing, together with predictions from Eq. (3) for a best fit set of parameter values – these are given in the caption. It can be seen that there is good agreement over the complete range of temperature and stress levels. Furthermore, these best fit parameter values correspond well in the case of  $n$  and  $Q$  to those obtained in §4 as an outcome of the analysis focussed solely on stage II behaviour – i.e. steady state strain rates. This is helpful and of course it’s certainly plausible that the activation energy and stress sensitivity could be similar in the primary and secondary parts of a given creep strain curve. Indeed, good agreement at longer times is only likely if the values of  $n$  and  $Q$  are similar to those obtained in the steady state analysis. Nevertheless, the fact that the primary sections of these curves can also be well-captured using these values is encouraging.

*6.2. Simulation of the indentation process*

Progression of indentation was simulated using the FEM formulation outlined in §3, with different sets of creep parameter values. Of course, a possible approach is to assume that, in all volume elements, the steady state creep rate (Eq. (2)) is instantaneously adopted, corresponding to the local stress (and temperature), and is maintained for the duration of each time increment. This procedure thus takes account of the (changing) stress field within the specimen, but takes no account of primary creep (or indeed of any effect of prior strain on the strain rate).

The outcome of such a simulation (using the steady state creep parameter values in the caption of Fig. 2) is shown in Fig. 7, for two sets of experimental output data corresponding to plots of the type shown in Fig. 4. One set concerns the load required to reach a penetration depth of  $2 \mu\text{m}$  during the load increase phase and the other relates to the further penetration occurring by the end of the dwell period, with both of these being examined as a



**Fig. 7.** Comparisons, for the four temperatures, between experimental data and predictions obtained using the FEM model, assuming that the steady state creep rates shown as predicted gradients in the plots of Fig. 2 applied in all volume elements throughout. The output data are: (a) the load required for the indenter to reach an initial depth of  $2 \mu\text{m}$  and (b) the further penetration during a 1-h dwell at this load, both as a function of the (imposed) rate of load increase during the initial period.

function of the rate of load increase. (The first of these outputs is particularly sensitive to the early part of the creep strain history, whereas the second is expected to be more dependent on slightly later portions – although, even in that case, the sensitivity to the initial creep rate is likely to be quite high, since the creep strain field is continually expanding.)

It can be seen in Fig. 7 that the predictions fail to capture the key elements of the experimental behaviour. In particular, it is predicted that neither of the outputs show any sensitivity to loading rate, whereas in practice there is a relatively strong dependence, particularly at the lower end of the range. This is clearly due to severe under-prediction of creep strain rates. It's evident that this is arising from neglect of primary creep. When primary creep is incorporated into the modelling, the agreement with experiment is improved. For example, Fig. 8 shows corresponding plots to those of Fig. 7, with Eq. (4) being employed in the FEM model, using the set of creep parameter values shown in Fig. 6. It can be seen that the sensitivity to loading rate is now reasonably well captured.

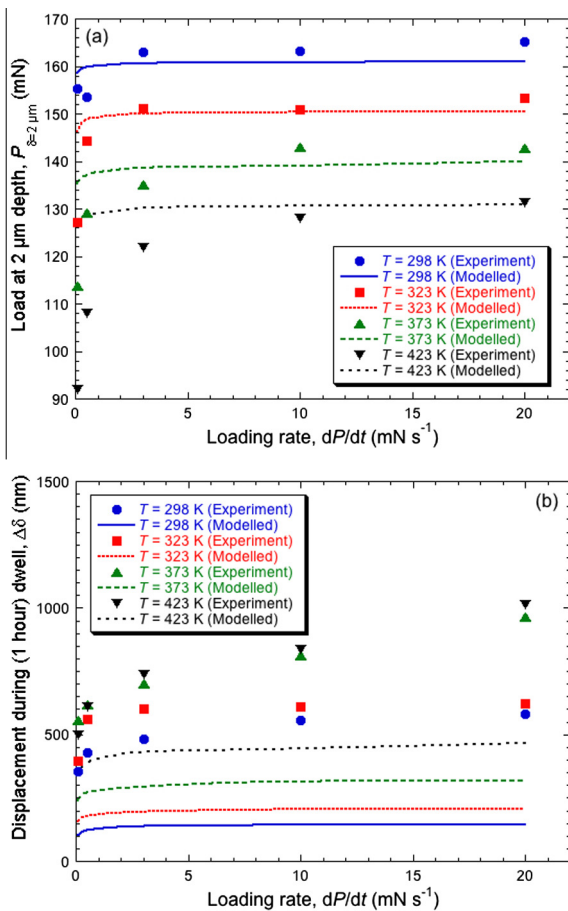


**Fig. 8.** Comparisons, for the four temperatures, between experimental and predicted outputs of the same type as in Fig. 7. Predictions were obtained using the FEM model, with the creep behaviour represented by Eq. (4) and Fig. 1, for the same set of parameter values as was used in Fig. 6 ( $C = 1.5 \cdot 10^6$  MPa $^{-n}$  s $^{-(m+1)}$ ,  $m = -0.5$ ,  $n = 1.47$  and  $Q = 13.4$  kJ mol $^{-1}$ ).

Of course, if indentation testing were being employed to characterise the creep response in the absence of prior information, then an iterative process would need to be carried out (based on chosen outputs, such as those being employed here) and a best fit set of parameter values would be obtained. The procedures by which such optimisation could be tackled, and indeed the outputs selected for comparison (and the functional form of the modelled creep curve), can all be adapted to suit particular objectives and other aspects of the case concerned. In the present work, some iterative optimisation was carried out, although it was not a comprehensive or systematic process, and it was focussed on the stress exponent. This was done in view of the fact that Fig. 8 indicates that the predicted dependence on temperature is in good agreement with experiment, so it appeared unnecessary to change the value of  $Q$ . The outcome is shown in Fig. 9, corresponding to the set of creep parameter values shown in the caption. It can be seen that the agreement is markedly better than in Fig. 8, although, understandably, it's not perfect. The most significant point to note here is that the creep

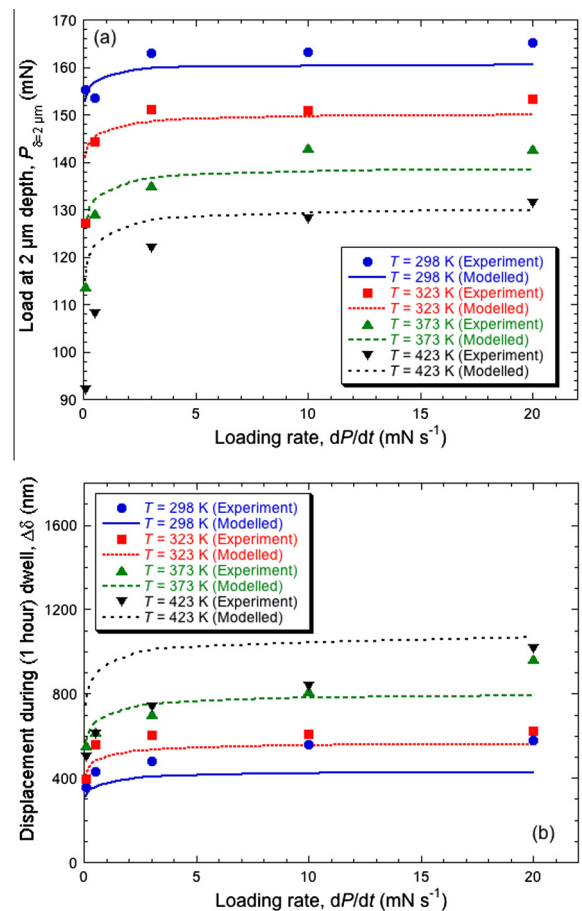


**Fig. 9.** Comparisons, for the four temperatures, between experimental and predicted outputs of the same type as in Fig. 7. Predictions were obtained using the FEM model, with the creep behaviour represented by Eq. (4) and Fig. 1, for the following set of parameter values:  $C = 1.5 \cdot 10^6$  MPa $^{-n}$  s $^{-(m+1)}$ ,  $m = -0.5$ ,  $n = 1.71$  and  $Q = 13.4$  kJ mol $^{-1}$ .

parameters that would have been obtained via this optimisation are close (i.e. within  $\sim 10\text{--}20\%$ ) to those derived from macroscopic (uniform stress field) testing. This is certainly encouraging, although it must be recognised that prior knowledge of the latter set of values inevitably had an influence on the iterative optimisation process carried out with the indentation data. It's clear that, in order to examine the usefulness of the procedure more rigorously, studies should be carried out based solely on indentation testing, involving material with completely unknown creep characteristics, and these are currently being instigated.

It is perhaps worth noting that, during study of creep via indentation, not only is primary creep likely to have a strong influence on the observed behaviour, but there will always tend to be regions (close to the indenter) in which the (deviatoric) stress is relatively high – i.e. close to the yield stress for the temperature concerned. Furthermore, depending on the sensitivity of the creep strain rate to stress, the measured response is likely to be quite strongly affected by what happens in these regions. The methodology, and indeed any methodology for the extraction of creep parameters from indentation data, may therefore be rather unsuitable for study of what might be termed a “low stress” regime of creep.

## 7. Conclusions

The following conclusions can be drawn from this work.

- (a) Nanoindentation has been carried out on extruded copper samples, for periods of one hour, over a range of temperature (between ambient and  $150\text{ }^{\circ}\text{C}$ ). The material concerned has been comprehensively characterised in terms of plasticity and creep behaviour over this temperature range, using conventional (uniform stress field) testing procedures. This creep behaviour, covering both primary and secondary regimes, has been characterised using a previously-proposed functional form for the creep strain history, with a best fit set of parameter values. The focus of the paper is to explore whether such parameter values can be obtained solely from experimental indentation data, via iterative usage of an FEM indentation model.
- (b) Displacement–time plots during indentation often appear to enter a steady state quite quickly, such that the velocity becomes approximately constant. By identifying “effective” stresses, strains and strain rates within the material, and employing a similar analysis to that applied to the steady state portion of a conventional creep curve, it is in principle possible to evaluate corresponding steady state creep parameters. In practice, the procedure is known to be unreliable and this has been highlighted by attempting to apply it to the copper indentation data, with the outcome being inconsistent and inaccurate.
- (c) There are two main probable causes of the unreliability outlined above. Firstly, the stress and strain fields under an indenter are far from being uniform and, secondly, primary creep is likely to have a

strong influence on the observed behaviour. In order to explore the relative importance of these two effects, an FEM process model was employed, with steady state creep rates assumed to be instantaneously adopted in all volume elements. This approach thus addressed the first source of error, but not the second. Comparisons were made between prediction and experiment for two output parameters – the load needed to reach a prescribed depth and the indenter penetration during a one hour dwell with this load, both as a function of loading rate. The predictions failed to capture the observed (relatively high) dependence of these outputs on loading rate (particularly at relatively low loading rates), and it's therefore clear that there was a severe under-prediction of creep rates (due to neglect of primary creep). This illustrated the importance of the primary creep behaviour.

- (d) By using the FEM model in conjunction with an analytical expression representing the complete creep curve, in combination with an assumption that the prior strain defines the starting point on the curve concerned within each volume element, predictions were obtained for the above two outputs. These showed fairly good agreement with experiment, using values for the creep curve parameters obtained from conventional creep testing. Better agreement was obtained by using a slightly different set of values and the effect of these changes gives an indication of the sensitivities involved. It is tentatively concluded that, for material with unknown creep characteristics, the proposed methodology could be used to evaluate creep parameter values with an estimated reliability of something like  $\pm 10\text{--}20\%$ , which is regarded as an encouraging outcome. The methodology could be refined by using alternative functional forms for the creep strain curve, outputs for comparison and iterative procedures to obtain a best fit set of parameter values. The results presented here could be taken as suggesting that similar values of the activation energy and the stress exponent are appropriate in both primary and secondary parts of the creep strain curve, at least for the copper employed in this work.

## Acknowledgements

Financial support for this work has been provided by AWE.

## References

- Dean, J., Wheeler, J.M., Clyne, T.W., 2010a. Use of quasi-static nanoindentation data to obtain stress-strain characteristics for metallic materials. *Acta Mater.* 58, 3613–3623.
- Dean, J., Aldrich-Smith, G., Clyne, T.W., 2010b. Use of nanoindentation to measure residual stresses in surface layers. *Acta Mater.* 59, 2749–2761.
- Chudoba, T., Richter, F., 2001. Investigation of creep behaviour under load during indentation experiments and its influence on hardness and modulus results. *Surf. Coat. Technol.* 148, 191–198.

- Seltzer, R., Mai, Y., 2008. Depth sensing indentation of linear viscoelastic-plastic solids: A simple method to determine creep compliance. *Eng. Fract. Mech.* 75, 4852–4862.
- Stone, D., Jakes, J., Puthoff, J., Elmustafa, A., 2010. Analysis of indentation creep. *J. Mat. Res.* 25, 611–621.
- Galli, M., Oyen, M., 2009. Creep properties from indentation tests by analytical and numerical techniques. *Int. J. Mat. Res.* 100, 954–959.
- Cao, Y., 2007. Determination of the creep exponent of a power-law creep solid using indentation tests. *Mech. Time-Depend. Mater.* 11, 159–172.
- Goodall, R., Clyne, T.W., 2006. A critical appraisal of the extraction of creep parameters from nanoindentation data obtained at room temperature. *Acta Mater.* 54, 5489–5499.
- Chen, W., Cheng, Y., Li, M., 2010. Indentation of power law creep solids by self-similar indenters. *Mat. Sci. Eng. A* 527, 5613–5618.
- Takagi, H., Dao, M., Fujiwara, M., 2008. Analysis on pseudo-steady indentation creep. *Acta Mech. Solida Sin.* 21, 283–288.
- Stone, D., Elmustafa, A., 2008. Analysis of indentation creep. In: *Proc. MRS (Fundamentals of Nanoindentation and Nanotribology IV)*, vol. 1049, pp. 163–68.
- Mulhearn, T.O., Tabor, D., 1960. Creep and hardness of metals: a physical study. *J. Inst. Met.* 89, 7–12.
- Fujiwara, M., Otsuka, M., 2001. Indentation creep of beta-Sn and Sn–Pb eutectic alloy. *Mater. Sci. Eng. A* A319–321, 929–933.
- Liu, H., Chen, Y., Tang, Y., Wei, S., Nuiu, G., 2007a. Tensile and indentation creep behaviour of Mg-5%Sn and Mg-5%Sn-2%Di alloys. *Mater. Sci. Eng. A* 464, 124–128.
- Liu, Y.J., Zhao, B., Xu, B.X., Yue, Z.F., 2007. Experimental and numerical study of the method to determine the creep parameters from the indentation creep testing. *Mater. Sci. Eng. A* 456, 103–108.